The nature of the intermolecular interaction between cobalt centers is still in question. The formation of $(Co(CN)_5)_2^{6-}$ complexes in one large cavity seems unlikely since this would require a large molecule with a total charge of −6 to be accommodated. The presence of charge-balancing cations, beyond those needed to balance the framework charge, would also be needed and would further crowd the cavity. The size of the dimer molecules alone would push the limits of the zeolite cage, and this crowding would be worsened by the extra cations needed to balance the −6 charge. The absence of any experimental evidence for dimer formation in the presence or absence of O_2 also suggests that this does not occur. A more reasonable explanation is the interaction of two cobalt centers in separate large cavities through the interconnecting channels. This would allow the oxidation to readily occur in materials where the mobility of $Co(CN)_5^{3-}$ is unrestricted, as is the case in CoNa-Y. The presence of cesium sterically inhibits a portion of the cobalt centers from interacting and stabilizes $Co(CN)_5^{3-}$.

Preparation of CsClCo(CN)-Y (sample F) under Ar was also repeated. The IR spectrum for the resulting material was identical to that prepared in air. Gas uptake measurements, however, show that this material actually has more active cobalt when prepared in air. This suggests that oxygen does not hamper the formation of $Co(CN)_5^{3-}$ but may even aid in its formation. This most likely occurs because oxygen can occupy the sixth coordination site and prevent the reaction with water shown in eq 4. The K_{O_2} value for this material (sample F) is 6.8 ± 3.3 $Torr^{-1}$.

Sample G, prepared in the presence of O_2, further demonstrates that the formation of the cobalt–O_2 adduct increases the amount of the O_2-binding species in the synthesis. Pressure absorption data taken on this sample show the active cobalt concentration to be 43 ± 4 μmol g^{-1}, and a K_{O_2} of 18 ± 2 $Torr^{-1}$ is found.

Conclusions about CsCo(CN)-Y. The presence of cesium in Co-Y prior to the addition of cyanide stabilizes $Co(CN)_5^{3-}$ inside zeolite Y by inhibiting the oxidation of cobalt(II) to $Co(CN)_6^{3-}$. It was shown in the study of Co(CN)Na-Y that this oxidation is driven by a high CN:Co ratio and most likely occurs through an intermolecular reaction of two $Co(CN)_5^{3-}$ complexes with water. Due to its large size, cesium appears to shield $Co(CN)_5^{3-}$ complexes from each other and inhibits their oxidation. In our best synthesis, a K_{O_2} of 18 ± 2 $Torr^{-1}$ has been measured with an active cobalt concentration of 43 ± 4 μmol g^{-1}. The large affinity this complex has for O_2 results in a material which is highly selective for absorbing O_2. A separation factor above 5000 has been calculated for O_2 absorption from a mixture of O_2 and N_2.

Registry No. $CoCl_2$, 7646-79-9; CsCl, 7647-17-8; CsOH, 21351-79-1; NaCN, 143-33-9; O_2, 7782-44-7; $Co(CN)_5^{3-}$, 14971-18-7; $Co(CN)_5(O_2)^{3-}$, 45044-10-8.

Contribution from the Department of Chemistry,
Purdue University, West Lafayette, Indiana 47907

Two-Electron Reduction of Carbon Disulfide at a Triply Bonded Dirhenium(II) Center with Preservation of the Dimetal Unit

Ju-Sheng Qi, Paul W. Schrier, Phillip E. Fanwick, and Richard A. Walton*

Received May 15, 1991

The triply bonded dirhenium(II) complexes $Re_2X_4(dppm)_2$ (X = Cl, Br; dppm = $Ph_2PCH_2PPh_2$) and $Re_2Br_4(dpam)_2$ (dpam = $Ph_2AsCH_2AsPh_2$) react with CS_2 via a 2-electron redox process to afford the dirhenium(III) compounds $Re_2(\mu\text{-}S)(\mu\text{-}X)X_3(CS)(\mu\text{-}LL)_2$ (LL = dppm, dpam) which may be derivatized by reaction with $TlPF_6$ in the presence of various monodentate ligands L′ to give the salts $[Re_2(\mu\text{-}S)(\mu\text{-}X)X_2(CS)(\mu\text{-}LL)_2(L')]PF_6$, where L′ = CH_3CN, C_2H_5CN, 4-$CH_3C_6H_4CN$, *t*-BuNC, or xylylNC. A single-crystal X-ray structure analysis of $[Re_2(\mu\text{-}S)(\mu\text{-}Br)Br_2(CS)(\mu\text{-}dpam)_2(NCC_2H_5)]PF_6\cdot CH_2Cl_2$ (**1**) shows the Re-Re distance to be unexpectedly long (2.956 (2) Å), a value that is intermediate between those of the dirhenium(III) complexes $Re_2(\mu\text{-}Cl)_2Cl_4(dppe)_2$ (no Re–Re bond) and $Re_2(\mu\text{-}Cl)_2Cl_4(\mu\text{-}dppm)_2$ (Re–Re double bond). Crystal data for **1** at 20 °C: triclinic space group $P\bar{1}$, $a = 12.653$ (2) Å, $b = 16.901$ (7) Å, $c = 17.368$ (7) Å, $\alpha = 65.88$ (4)°, $\beta = 78.91$ (2)°, $\gamma = 72.12$ (3)°, $V = 3216$ (2) $Å^3$, and $Z = 2$. The structure was refined to $R = 0.062$ ($R_w = 0.073$) for 3786 data with $I > 3\sigma(I)$.

Introduction

One of the reaction pathways often encountered in the interaction of carbon disulfide with metal complexes[1] is its insertion into metal–hydride,[2] metal–halide,[3] metal–alkyl,[4] and metal–dialkylamido[5] ligand bonds. Redox reactions can also occur, and these include the reductive dimerization of CS_2 (in head-to-head or head-to-tail fashions)[6] as well as its reductive cleavage to give sulfido and carbon monosulfide fragments.[1,7-9] The latter reaction course proceeds via a CS_2 adduct and may or may not give a final product in which *both* S^{2-} and CS are incorporated into the *same* metal-containing species.[1,7-9] The latter features are quite well defined in mononuclear and polynuclear platinum chemistry. For example, one such reaction is the formation of $Pt_2Cl_2(\mu_2\text{-}\eta^2\text{-}CS_2)(\mu\text{-}dppm)_2$ (dppm = $Ph_2PCH_2PPh_2$) from $Pt_2Cl_2(\mu\text{-}dppm)_2$ and excess CS_2.[10] On the other hand, the reaction of the mononuclear complex $Pt(\eta^2\text{-}CS_2)(dppe)_2$ (dppe = $Ph_2PCH_2CH_2PPh_2$) with $Pt(\eta^2\text{-}C_2H_4)(PPh_3)_2$ yields the diplatinum complex (dppe)$Pt(\mu\text{-}S)Pt(PPh_3)_2(CS)$ through the 2-electron reduction of CS_2.[11] The oxidative addition of CS_2 to trinuclear Pt clusters has also been reported,[9] although in some of these instances cluster degradation can occur.[12,13] We now report the first examples of the 2-electron reduction of CS_2 by a multiply bonded dimetal complex.[14] We find that the triply bonded dirhenium(II) complexes

---

(1) A recent review of much of the chemistry emanating from the reactions of metal complexes with carbon disulfide is available: Broadhurst, P. V. *Polyhedron* **1985**, *4*, 1801.

(2) See, for example: Schauer, S. J.; Eyman, D. P.; Bernhardt, R. J.; Wolff, M. A.; Mallis, L. M. *Inorg. Chem.* **1991**, *30*, 570 and references cited therein.

(3) Jentsch, D.; Jones, P. G.; Thone, C.; Schwarzmann, E. *J. Chem. Soc., Chem. Commun.* **1989**, 1495.

(4) Darensbourg, D. J.; Wiegreffe, H. P.; Reibenspies, J. H. *Organometallics* **1991**, *10*, 6.

(5) Ziegler, M. L.; Blechschmitt, K.; Bock, H.; Guggolz, E.; Korswagen, R. P. *Z. Naturforsch.* **1988**, *43B*, 590.

(6) See, for example: Carmona, E.; Galindo, A.; Monge, A.; Munoz, M. A.; Poveda, M. L.; Ruiz, C. *Inorg. Chem.* **1990**, *29*, 5074 and references cited therein.

(7) Baird, M. C.; Wilkinson, G. *J. Chem. Soc. A* **1967**, 865.

(8) Werner, H.; Ebner, M.; Otto, H. *J. Organomet. Chem.* **1988**, 350.

(9) Bradford, A. M.; Jennings, M. C.; Puddephatt, R. J. *Organometallics* **1989**, *8*, 2367.

(10) Cameron, T. S.; Gardner, P. A.; Grundy, K. R. *J. Organomet. Chem.* **1981**, *212*, C19.

(11) Hawling, W. M.; Walker, A.; Woitzik, M. A. *J. Chem. Soc., Chem. Commun.* **1983**, 11.

(12) Farrar, D. H.; Gukathasan, R. R.; Morris, S. A. *Inorg. Chem.* **1984**, *23*, 3258.

(13) Browning, C. S.; Farrar, D. H.; Gukathasan, R. R.; Morris, S. A. *Organometallics* **1985**, *4*, 1750.

(14) The addition of CS_2 to the triply bonded dimolybdenum compounds $(\eta^5\text{-}C_5R_5)_2Mo_2(CO)_4$ (R = H, CH_3) has been reported to yield a η^2-CS_2 complex, but there is no evidence for an ensuing redox reaction; see: Brunner, H.; Meier, W.; Wachter, J. *J. Organomet. Chem.* **1981**, *210*, C23.

0020-1669/92/1331-0258$03.00/0

$Re_2X_4(dppm)_2$ (X = Cl, Br)[15] and $Re_2Br_4(dpam)_2$ (dpam = $Ph_2AsCH_2AsPh_2$)[16] react to give the stable, edge-shared bioctahedral dirhenium(III) species $Re_2(\mu\text{-}S)(\mu\text{-}X)X_3(CS)(\mu\text{-}dppm)_2$ (X = Cl, Br) and $Re_2(\mu\text{-}S)(\mu\text{-}Br)Br_3(CS)(\mu\text{-}dpam)_2$. The syntheses, spectroscopic properties, structures, and certain reactivity studies are described in the present report.

Experimental Section

Starting Materials. The compounds $Re_2X_4(dppm)_2$ (X = Cl, Br)[15a] and $Re_2Br_4(dpam)_2$[16] were prepared according to established literature procedures. All solvents were obtained from commercial sources and were used as received. Syntheses were performed with the use of an atmosphere of dry nitrogen, and solvents were deoxygenated prior to use.

A. Synthesis of $Re_2(\mu\text{-}S)(\mu\text{-}X)X_3(CS)(dppm)_2$ (X = Cl, Br). (i) X = Cl. A suspension of $Re_2Cl_4(dppm)_2$ (0.200 g, 0.156 mmol) was stirred in CS_2 (15 mL) for 1 day. An olive green solid was filtered off, washed with diethyl ether (2 × 15 mL), and vacuum-dried; yield 0.152 g (72%). Anal. Calcd for $C_{51}H_{44}Cl_4P_4Re_2S_2$: C, 45.07; H, 3.27; Cl, 10.43. Found: C, 44.81; H, 3.62; Cl, 10.52.

(ii) X = Br. This complex was prepared in 80% yield by the use of a procedure similar to that described for its chloride analogue. Anal. Calcd for $C_{51}H_{44}Br_4P_4Re_2S_2$: C, 39.85; H, 2.89; Br, 20.80. Found: C, 39.89; H, 3.17; Cl, 20.97.

B. Synthesis of $Re_2(\mu\text{-}S)(\mu\text{-}Br)Br_3(CS)(dpam)_2$. A quantity of $Re_2Br_4(dpam)_2$ (0.200 g, 0.122 mmol) was stirred in CS_2 (15 mL) for 1 day. The resulting dark green solid was filtered off, washed with diethyl ether (2 × 15 mL), and vacuum-dried; yield 0.158 g (75%). Anal. Calcd for $C_{51}H_{44}As_4Br_4Re_2S_2$: C, 35.76; H, 2.59. Found: C, 35.11; H, 2.48.

C. Synthesis of $[Re_2(\mu\text{-}S)(\mu\text{-}Cl)Cl_2(CS)(dppm)_2(NCR)]PF_6$. (i) R = CH_3. A mixture of $Re_2(\mu\text{-}S)(\mu\text{-}Cl)Cl_3(CS)(dppm)_2$ (0.100 g, 0.074 mmol) and $TlPF_6$ (0.026 g, 0.074 mmol) was stirred in CH_2Cl_2 (10 mL). After 10 min, 1 mL of CH_3CN was added, and the solution was stirred for an additional hour. The dark green mixture was filtered to remove TlCl, and the filtrate was layered with excess diethyl ether and kept at 0 °C for 12 h. A crop of dark green needles was filtered off and washed with diethyl ether (15 mL) and vacuum-dried; yield 0.083 g (74%). Anal. Calcd for $C_{53}H_{47}Cl_3F_6NP_5Re_2S_2$: C, 42.17; H, 3.14. Found: C, 42.21; H, 3.31.

Similar procedures to this were used to obtain the following dark green nitrile derivatives.

(ii) R = CH_2CH_3. Yield: 85%. Anal. Calcd for $C_{54}H_{49}Cl_3F_6NP_5Re_2S_2$: C, 42.56; H, 3.25. Found: C, 41.61; H, 3.36.

(iii) R = C_6H_4-4-CH_3. Yield: 75%. Anal. Calcd for $C_{59}H_{51}Cl_3F_6NP_5Re_2S_2$: C, 44.68; H, 3.25. Found: C, 43.86; H, 3.30.

D. Synthesis of $[Re_2(\mu\text{-}S)(\mu\text{-}Br)Br_2(CS)(dppm)_2(NCR)]PF_6$. (i) R = CH_3. A mixture of $Re_2(\mu\text{-}S)(\mu\text{-}Br)Br_3(CS)(dppm)_2$ (0.100 g, 0.065 mmol) and $TlPF_6$ (0.025 g, 0.070 mmol) was stirred for 10 min in 10 mL of CH_2Cl_2. Next, 1 mL of CH_3CN was added, and the solution was stirred for an additional 30 min. The resulting dark green mixture was filtered to remove TlBr, and diethyl ether (50 mL) was added to the filtrate to initiate precipitation. After the filtrate had been kept at 0 °C for 1 h, a dark green powder was collected by filtration, washed with diethyl ether (15 mL), and vacuum-dried; yield 0.083 g (78%). Anal. Calcd for $C_{53}H_{47}Br_3F_6NP_5Re_2S_2$: C, 38.74; H, 2.89. Found: C, 39.11; H, 3.16.

A similar procedure was used to prepare the following dark green nitrile derivatives.

(ii) R = CH_2CH_3. Yield: 78%. Anal. Calcd for $C_{55}H_{51.5}Br_3F_6NO_{0.25}P_5Re_2S_2$ (i.e. $[Re_2SBr_3(CS)(dppm)_2(NCC_2H_5)]PF_6{\cdot}0.25(C_2H_5)_2O$): C, 39.42; H, 3.10. Found: C, 39.66; H, 3.45. The presence of lattice diethyl ether was confirmed by ^1H NMR spectroscopy.

(iii) R = C_6H_4-4-CH_3. Yield: 41%. Anal. Calcd for $C_{59}H_{51}Br_3F_6NP_5Re_2S_2$: C, 41.22; H, 2.99. Found: C, 41.09; H, 3.44.

E. Synthesis of $[Re_2(\mu\text{-}S)(\mu\text{-}Br)Br_2(CS)(dpam)_2(NCR)]PF_6$. (i) R = CH_3. A solution that contained $Re_2(\mu\text{-}S)(\mu\text{-}Br)Br_3(CS)(dpam)_2$ (0.100 g, 0.055 mmol) and $TlPF_6$ (0.019 g, 0.055 mmol) dissolved in CH_2Cl_2 (10 mL) was stirred for 10 min. Next, 1 mL of CH_3CN was added, and stirring continued for 1 h. The dark green mixture was filtered to remove TlBr, and the filtrate was layered with diethyl ether and cooled to 0 °C for 12 h. The resulting dark green needles were filtered off, washed with diethyl ether (15 mL), and vacuum-dried; yield 0.073 g (73%). Anal. Calcd for $C_{53}H_{47}As_4Br_3F_6NPRe_2S_2$: C, 35.00; H, 2.61. Found: C, 35.29; H, 2.70.

Table I. Crystallographic Data for $[Re_2(\mu\text{-}S)(\mu\text{-}Br)Br_2(CS)(\mu\text{-}dpam)_2(NCC_2H_5)]PF_6{\cdot}CH_2Cl_2$ (**1**)

chem formula	$Re_2Br_3As_4Cl_2S_2PF_6NC_{55}H_{51}$
fw	1917.84
space group	$P\bar{1}$ (No. 2)
a, Å	12.653 (2)
b, Å	16.901 (7)
c, Å	17.368 (7)
α, deg	65.88 (4)
β, deg	78.91 (2)
γ, deg	72.12 (3)
V, Å^3	3216 (2)
Z	2
T, °C	20
λ(Mo Kα), Å	0.71073
ρ_{calcd}, g cm^{-3}	1.981
μ(Mo Kα), cm^{-1}	79.17
transm coeff	1.00–0.40
R^a	0.062
$R_w{}^b$	0.073

$^a R = \sum||F_o| - |F_c||/\sum|F_o|$. $^b R_w = \{\sum w(|F_o| - |F_c|)^2/\sum w|F_o|^2\}^{1/2}$; $w = 1/\sigma^2(|F_o|)$.

(ii) R = CH_2CH_3. With the use of a procedure similar to that used in section E(i), dark green crystals were obtained in 76% yield. Anal. Calcd for $C_{54}H_{49}As_4Br_3F_6NPRe_2S_2$: C, 35.38; H, 2.70. Found: C, 35.10; H, 2.79.

F. Synthesis of $[Re_2(\mu\text{-}S)(\mu\text{-}X)X_2(CS)(dppm)_2(CNR)]PF_6$. (i) X = Cl, R = *t*-Bu. A mixture of $Re_2(\mu\text{-}S)(\mu\text{-}Cl)Cl_3(CS)(dppm)_2$ (0.060 g, 0.044 mmol), $TlPF_6$ (0.015 g, 0.044 mmol), and *t*-BuNC (0.005 mL, 0.044 mmol) in CH_2Cl_2 (10 mL) was stirred at room temperature for 48 h. The resulting green reaction mixture was filtered to remove the white precipitate of TlCl, and the filtrate was evaporated to dryness. The residue was redissolved in a small volume of CH_2Cl_2 and filtered. The final product was obtained in crystalline form by the slow diffusion of hexane vapor into the CH_2Cl_2 solution of the complex over a 2-week period. The green crystals were washed with a 10-mL portion of diethyl ether and vacuum-dried; yield 0.060 g (90%). Anal. Calcd for $C_{56}H_{53}Cl_3F_6NP_5Re_2S_2$: C, 43.35; H, 3.44. Found: C, 43.75; H, 3.71.

(ii) X = Cl, R = xylyl. This complex was isolated in 38% yield with the use of a procedure similar to that in section F(i).

(iii) X = Br, R = xylyl. A mixture of $Re_2(\mu\text{-}S)(\mu\text{-}Br)Br_3(CS)(dppm)_2$ (0.100 g, 0.065 mmol), $TlPF_6$ (0.025 g, 0.065 mmol), and xylylNC (0.013 g, 0.100 mmol) in CH_2Cl_2 (10 mL) was stirred for 1 h. The dark green solution was filtered to remove TlBr, and the filtrate was treated with excess diethyl ether and kept at 0 °C for 3 h to afford a dark green powder. The product was filtered off, washed with toluene (15 mL) and diethyl ether (2 × 15 mL), and vacuum-dried; yield 0.061 g (54%). Anal. Calcd for $C_{60}H_{53}Br_3F_6NP_5Re_2S_2$: C, 41.58; H, 3.09. Found: C, 41.11; H, 3.21.

G. Synthesis of $[Re_2(\mu\text{-}S)(\mu\text{-}X)X_3(CS)(dppm)_2]PF_6$. (i) X = Cl. A solution of $Re_2(\mu\text{-}S)(\mu\text{-}Cl)Cl_3(CS)(dppm)_2$ (0.100 g, 0.074 mmol) and $[(\eta^5\text{-}C_5H_5)_2Fe]PF_6$ (0.025 g, 0.074 mmol) was stirred in CH_2Cl_2 (10 mL) for 1 h. The dark blue-green solution was reduced in volume to ca. 5 mL under vacuum, and 30 mL of diethyl ether was added to initiate precipitation. A dark blue-green powder was filtered off and washed with diethyl ether (2 × 15 mL) and vacuum-dried; yield 0.079 g (71%). Anal. Calcd for $C_{51}H_{44}Cl_4F_6P_5Re_2S_2$: C, 40.72; H, 2.95. Found: C, 40.59; H, 3.35.

This oxidation can also be accomplished through the use of a CH_2Cl_2 solution of $NOPF_6$.

(ii) X = Br. A mixture of $Re_2(\mu\text{-}S)(\mu\text{-}Br)Br_3(CS)(dppm)_2$ (0.100 g, 0.065 mmol) and $NOPF_6$ (0.012 g, 0.070 mmol) was stirred in CH_2Cl_2 (10 mL) for 15 min. A dark blue-green solution was reduced in volume to ca. 5 mL, and excess diethyl ether was added to precipitate a dark blue-green powder. The product was washed with diethyl ether (15 mL) and vacuum-dried; yield 0.098 g (90%). Anal. Calcd for $C_{51}H_{44}Br_4F_6P_5Re_2S_2$: C, 36.42; H, 2.64. Found: C, 36.39; H, 2.88.

Preparation of Single Crystals for Structure Determination. Crystals of $[Re_2(\mu\text{-}S)(\mu\text{-}Br)Br_2(CS)(dpam)_2(NCC_2H_5]PF_6{\cdot}CH_2Cl_2$ were grown by the slow diffusion of diisopropyl ether into a dichloromethane solution of the complex. Suitable dark green crystals were obtained after a period of approximately 1 week.

X-ray Crystallography. The structure of $[Re_2(\mu\text{-}S)(\mu\text{-}Br)Br_2(CS)(dpam)_2(NCC_2H_5)]PF_6{\cdot}CH_2Cl_2$ was determined at +20 °C by application of the standard procedures. The basic crystallographic parameters for this complex are listed in Table I. The cell constants are based on

---

(15) (a) Cutler, A. R.; Derringer, D. R.; Fanwick, P. E.; Walton, R. A. *J. Am. Chem. Soc.* **1988**, *110*, 5024. (b) Barder, T. J.; Cotton, F. A.; Dunbar, K. R.; Powell, G. L.; Schwotzer, W.; Walton, R. A. *Inorg. Chem.* **1985**, *24*, 2550. (c) Walton, R. A. *Polyhedron* **1989**, *8*, 1689.

(16) Costello, M. T.; Derringer, D. R.; Fanwick, P. E.; Price, A. C.; Rivera, M. I.; Scheiber, E.; Siurek, III, E. W.; Walton, R. A. *Polyhedron* **1990**, *9*, 573.

Table II. Positional Parameters and Equivalent Isotropic Displacement Parameters (Å^2) for the Non-Phenyl Atoms of the Cation of **1** and Their Estimated Standard Deviations[a]

atom	*x*	*y*	*z*	*B*
Re(1)	0.18100 (9)	0.74068 (8)	0.32167 (7)	2.42 (3)
Re(2)	0.32920 (9)	0.84985 (8)	0.20183 (7)	2.54 (3)
Br(1)	0.0137 (2)	0.6786 (2)	0.3404 (2)	4.6 (1)
Br(2)	0.3704 (3)	0.9452 (2)	0.0478 (2)	4.5 (1)
Br(B)	0.1665 (2)	0.8133 (2)	0.1636 (2)	3.67 (9)
As(11)	0.3052 (2)	0.5966 (2)	0.3089 (2)	2.71 (8)
As(12)	0.0415 (2)	0.8761 (2)	0.3426 (2)	3.11 (8)
As(21)	0.4641 (2)	0.7154 (2)	0.1747 (2)	2.83 (8)
As(22)	0.2038 (2)	0.9937 (2)	0.2171 (2)	3.08 (8)
S(2)	0.5535 (9)	0.9026 (7)	0.2329 (8)	7.7 (4)
S(12)	0.3236 (6)	0.7788 (5)	0.3442 (4)	2.9 (2)
N(1)	0.169 (2)	0.674 (2)	0.455 (2)	4.7 (6)*
C(2)	0.164 (2)	0.637 (2)	0.524 (2)	4.1 (7)*
C(3)	0.128 (4)	0.587 (3)	0.608 (3)	9 (1)*
C(4)	0.016 (4)	0.561 (3)	0.622 (3)	9 (1)*
C(2S)	0.462 (2)	0.885 (2)	0.215 (2)	5.8 (9)
C(B1)	0.460 (2)	0.604 (2)	0.270 (2)	3.2 (9)
C(B2)	0.111 (2)	0.972 (2)	0.324 (2)	3.1 (8)

[a] Starred values designate atoms that were refined isotropically. Values for anisotropically refined atoms are given in the form of the isotropic equivalent thermal parameter defined as $(4/3)[a^2\beta(1,1) + b^2\beta(2,2) + c^2\beta(3,3) + ab(\cos\gamma)\beta(1,2) + ac(\cos\beta)\beta(1,3) + bc(\cos\alpha)\beta(2,3)]$.

Table III. Important Bond Distances (Å) and Bond Angles (deg) for the $[Re_2(\mu\text{-}S)(\mu\text{-}Br)Br_2(CS)(\mu\text{-dpam})_2(NCC_2H_5)]^+$ Cation in the Structure of **1**[a]

Bond Distances			
Re(1)–Re(2)	2.956 (2)	Re(2)–As(21)	2.547 (4)
Re(1)–Br(1)	2.551 (4)	Re(2)–As(22)	2.548 (4)
Re(1)–Br(B)	2.526 (4)	Re(2)–S(12)	2.263 (8)
Re(1)–As(11)	2.532 (4)	Re(2)–C(2S)	2.02 (3)
Re(1)–As(12)	2.537 (4)	S(2)–C(2S)	1.40 (4)
Re(1)–S(12)	2.240 (8)	N(1)–C(2)	1.10 (4)
Re(1)–N(1)	2.12 (3)	C(2)–C(3)	1.42 (5)
Re(2)–Br(2)	2.546 (4)	C(3)–C(4)	1.56 (6)
Re(2)–Br(B)	2.590 (4)		
Bond Angles			
Re(2)–Re(1)–Br(1)	146.4 (1)	Re(1)–Re(2)–As(22)	92.4 (1)
Re(2)–Re(1)–Br(B)	55.72 (9)	Re(1)–Re(2)–S(12)	48.6 (2)
Re(2)–Re(1)–As(11)	93.07 (9)	Re(1)–Re(2)–C(2S)	134 (1)
Re(2)–Re(1)–As(12)	92.8 (1)	Br(2)–Re(2)–Br(B)	91.6 (1)
Re(2)–Re(1)–S(12)	49.3 (2)	Br(2)–Re(2)–As(21)	88.1 (1)
Re(2)–Re(1)–N(1)	133.7 (7)	Br(2)–Re(2)–As(22)	86.9 (1)
Br(1)–Re(1)–Br(B)	90.7 (1)	Br(2)–Re(2)–S(12)	166.0 (2)
Br(1)–Re(1)–As(11)	88.3 (1)	Br(2)–Re(2)–C(2S)	81 (1)
Br(1)–Re(1)–As(12)	86.2 (1)	Br(B)–Re(2)–As(21)	89.8 (1)
Br(1)–Re(1)–S(12)	164.2 (2)	Br(B)–Re(2)–As(22)	92.4 (1)
Br(1)–Re(1)–N(1)	79.9 (7)	Br(B)–Re(2)–S(12)	102.3 (2)
Br(B)–Re(1)–As(11)	91.2 (1)	Br(B)–Re(2)–C(2S)	172 (1)
Br(B)–Re(1)–As(12)	91.2 (1)	As(21)–Re(2)–As(22)	174.6 (1)
Br(B)–Re(1)–S(12)	105.0 (2)	As(21)–Re(2)–S(12)	93.8 (2)
Br(B)–Re(1)–N(1)	170.6 (7)	As(21)–Re(2)–C(2S)	88 (1)
As(11)–Re(1)–As(12)	174.1 (1)	As(22)–Re(2)–S(12)	90.5 (3)
As(11)–Re(1)–S(12)	92.7 (3)	As(22)–Re(2)–C(2S)	89 (1)
As(11)–Re(1)–N(1)	89.2 (8)	S(12)–Re(2)–C(2S)	85 (1)
As(12)–Re(1)–S(12)	92.0 (3)	Re(1)–Br(B)–Re(2)	70.57 (9)
As(12)–Re(1)–N(1)	87.6 (8)	Re(1)–S(12)–Re(2)	82.1 (3)
S(12)–Re(1)–N(1)	84.4 (8)	Re(1)–N(1)–C(2)	179 (3)
Re(1)–Re(2)–Br(2)	145.2 (1)	N(1)–C(2)–C(3)	162 (4)
Re(1)–Re(2)–Br(B)	53.70 (9)	C(2)–C(3)–C(4)	119 (4)
Re(1)–Re(2)–As(21)	92.84 (9)	Re(2)–C(2S)–S(2)	174 (3)

[a] Numbers in parentheses are estimated standard deviation in the least significant digits.

25 reflections with $13 < \theta < 17°$. Three standard reflections were measured after 5000 sec. of beam time during data collection; there were no systemmatic variations in intensity.

Calculations were performed on a MicroVAX II computer using the Enraf-Nonius structure determination package. Lorentz and polarization corrections were applied to the data. The structure was solved by the use of the Patterson heavy-atom method, which revealed the positions of the Re atoms. The remaining non-hydrogen atoms were identified in succeeding difference Fourier syntheses. The atoms of a molecule of lattice CH_2Cl_2 are located about a general position. Hydrogen atoms of the dpam and EtCN ligands were not included. An empirical absorption correction was applied,[17] but no correction for extinction was made. The structure was refined by full-matrix least-squares techniques where the function minimized was $\sum w(|F_o| - |F_c|)^2$, where w is the weighting factor defined as $w = 1/\sigma^2(F_o)$. All atoms of the dirhenium complex except those of the propionitrile ligand and the phenyl carbon atoms of the dpam ligand were refined anisotropically; corrections for anomalous scattering were applied to these atoms.[18]

Positional parameters and their errors for all atoms, except the phenyl group atoms and those of the lattice CH_2Cl_2 molecule, are listed in Table II. Important intramolecular bond distances and angles are given in Table III. Full details of the crystal data, data collection parameters, and all structural parameters are available as supplementary material.

Physical Measurements. Electrochemical and spectroscopic characterizations were carried out with the use of instrumentation and techniques described previously.[16]

Elemental microanalyses were performed by Dr. H. D. Lee of the Purdue Microanalytical Laboratory.

Results

The reactions of $Re_2X_4(dppm)_2$ (X = Cl, Br) and $Re_2Br_4(dpam)_2$ with neat CS_2 proceed in high yield according to eq 1.

$$Re_2X_4(LL)_2 + CS_2 \rightarrow Re_2SX_4(CS)(LL)_2 \qquad (1)$$

$$X = Cl, Br;\ LL = dppm, dpam$$

The presence of a terminal CS group is readily established by the observation of a single intense ν(CS) mode near 1290 cm^{-1} in the IR spectra (Nujol mulls) of the products (Table IV). The cyclic voltammograms (CV's) of solutions of these complexes in 0.1 M n-Bu_4NPF_6 in CH_2Cl_2 are very similar and show three reversible electrochemical processes at $E_{1/2}$(ox) ca. +1.4 V, $E_{1/2}$(ox) ca. +0.4 V, and $E_{1/2}$(red) ca. −0.4 V and an irreversible reduction at $E_{p,c}$ ca. −1.4 V vs Ag/AgCl. The accessibility and reversibility of the oxidation at ca. +0.4 V was demonstrated by the oxidation of the dppm complexes $Re_2SX_4(CS)(dppm)_2$ (X = Cl, Br) to the paramagnetic salts $[Re_2SX_4(CS)(dppm)_2]PF_6$ through the use of $[(\eta^5\text{-}C_5H_5)_2Fe]PF_6$ or $NOPF_6$ as oxidant (eq 2). Oxidation

$$Re_2SX_4(CS)(dppm)_2 + [ox]PF_6 \xrightarrow{CH_2Cl_2} [Re_2SX_4(CS)(dppm)_2]PF_6 + red \qquad (2)$$

$$[ox]^+ = [(\eta^5\text{-}C_5H_5)_2Fe]^+ \text{ or } [NO]^+$$

$$red = (\eta^5\text{-}C_5H_5)_2Fe \text{ or } NO$$

is accompanied by a shift in the ν(CS) mode of ca. +30 cm^{-1}. The CV's of the salts are the same as those of their neutral precursors except that the process at ca. +0.4 V is now a one-electron reduction. A solution of $[Re_2SCl_4(CS)(dppm)_2]PF_6$ in dichloromethane has a magnetic moment of 1.75(±0.05) as determined by the Evans method. The X-band ESR spectra of the chloride and bromide complexes (recorded in CH_2Cl_2/toluene at −160 °C) each exhibit a complex signal centered at $g \approx 2.03$, showing poorly resolved hyperfine structure.

While the green, diamagnetic $Re_2SX_4(CS)(LL)_2$ complexes generally have low solubility in common organic solvents, their solubility is enhanced considerably following their derivatization as shown in eq 3. These reactions proceed readily in the case

$$Re_2SX_4(CS)(LL)_2 + L' + TlPF_6 \rightarrow [Re_2SX_3(CS)(LL)_2L']PF_6 + TlX \qquad (3)$$

$$X = Cl, Br;\ LL = dppm, dpam$$

of L′ = CH_3CN, C_2H_5CN, 4-$CH_3C_6H_4CN$, t-BuNC, and xylylNC, although not all possible compounds have been prepared. Those that have are listed in Table IV, along with their IR spectral data and the CV data for their solutions in 0.1 M n-Bu_4NPF_6 in CH_2Cl_2. The ν(CS) modes are shifted to higher frequencies by

---

[17] Walker, N.; Stuart, D. *Acta Crystallogr., Sect. A: Found. Crystallogr.* **1983**, *A39*, 158.

[18] Cromer, D. T. *International Tables for X-ray Crystallography*; Kynoch: Birmingham, England, 1974; Vol. IV, Table 2.3.1. (b) For the scattering factors used in the structure solution see: Cromer, D. T.; Waber, J. T. *Ibid.*, Table 2.2B.

Table IV. Infrared Spectral Properties and Cyclic Voltammetric Data for Products from the Reactions of Carbon Disulfide with $Re_2X_4(LL)_2$ (X = Cl, Br; LL = dppm, dpam)

complex	IR,[a] cm^{-1}		CV half-wave potentials,[b] V				
	ν(CN)	ν(CS)	$E_{1/2}$-(ox)(2)	$E_{1/2}$-(ox)(1)	$E_{1/2}$-(red)(1)	$E_{1/2}$-(red)(2)	$E_{1/2}$-(red)(3)
$Re_2(\mu\text{-}S)(\mu\text{-}Cl)Cl_3(CS)(dppm)_2$		1291 vs	+1.40	+0.40	−0.45	−1.50[d]	
$Re_2(\mu\text{-}S)(\mu\text{-}Br)Br_3(CS)(dppm)_2$		1287 vs	+1.42	+0.46	−0.45	−1.27[d]	
$Re_2(\mu\text{-}S)(\mu\text{-}Br)Br_3(CS)(dpam)_2$		1284 vs	+1.39	+0.47	−0.35	−1.47	
$[Re_2(\mu\text{-}S)(\mu\text{-}Cl)Cl_3(CS)(dppm)_2]PF_6$		1322 vs	+1.40	+0.43[c]	−0.47	−1.45[d]	
$[Re_2(\mu\text{-}S)(\mu\text{-}Br)Br_3(CS)(dppm)_2]PF_6$		1316 vs	+1.40	+0.46[c]	−0.46	−1.26[d]	
$[Re_2(\mu\text{-}S)(\mu\text{-}Cl)Cl_2(CS)(dppm)_2(NCCH_3)]PF_6$	2180 vw	1309 vs		+0.80	−0.32	−0.98[d]	−1.31
$[Re_2(\mu\text{-}S)(\mu\text{-}Cl)Cl_2(CS)(dppm)_2(NCC_2H_5)]PF_6$	2175 vw	1312 vs		+0.80	−0.31	−0.97[d]	−1.31
$[Re_2(\mu\text{-}S)(\mu\text{-}Cl)Cl_2(CS)(dppm)_2(NCC_6H_4\text{-}4\text{-}CH_3)]PF_6$	2222 w	1312 vs		+0.78	−0.26	−0.86[d]	−1.27
$[Re_2(\mu\text{-}S)(\mu\text{-}Br)Br_2(CS)(dppm)_2(NCCH_3)]PF_6$	2192 vw	1314 vs		+0.84	−0.28	−0.84[d]	−1.28
$[Re_2(\mu\text{-}S)(\mu\text{-}Br)Br_2(CS)(dppm)_2(NCC_2H_5)]PF_6$	2190 vw	1315 vs		+0.81	−0.31	−0.87[d]	−1.31
$[Re_2(\mu\text{-}S)(\mu\text{-}Br)Br_2(CS)(dppm)_2(NCC_6H_4\text{-}4\text{-}CH_3)]PF_6$	2228 w	1308 vs		+0.81	−0.29	−0.77[d]	−1.25
$[Re_2(\mu\text{-}S)(\mu\text{-}Cl)Cl_2(CS)(dppm)_2(CN\text{-}t\text{-}Bu)]PF_6$	2179 vs	1310 vs		+0.91	−0.28	−0.84	−1.23
$[Re_2(\mu\text{-}S)(\mu\text{-}Cl)Cl_2(CS)(dppm)_2(CNxyl)]PF_6$	2138 s	1308 vs		+0.88	−0.19	−0.73	−1.29
$[Re_2(\mu\text{-}S)(\mu\text{-}Br)Br_2(CS)(dppm)_2(CNxyl)]PF_6$	2130 s	1308 vs		+0.95	−0.18	−0.68	−1.18
$[Re_2(\mu\text{-}S)(\mu\text{-}Br)Br_2(CS)(dpam)_2(NCCH_3)]PF_6$	2178 vw	1310 vs		+0.79	−0.20	−0.82	−1.29
$[Re_2(\mu\text{-}S)(\mu\text{-}Br)Br_2(CS)(dpam)_2(NCC_2H_5)]PF_6$	2176 vw	1314 vs		+0.78	−0.20	−0.84	−1.32

[a] Recorded as Nujol mulls. Complexes that contain PF_6^- all show a characteristic absorption due to ν(P–F) beween 845 and 837 cm^{-1}. [b] Measured on 0.1 M TBAH in CH_2Cl_2 solutions and referenced to the Ag/AgCl electrode, with a scan rate (v) of 200 mV/s at a Pt-bead electrode. Under our experimental conditions $E_{1/2}$ for the ferrocenium/ferrocene couple was +0.47 V vs Ag/AgCl. For the processes $E_{1/2}$(ox)(1), $E_{1/2}$(red)(1), $E_{1/2}$-(red)(2), and $E_{1/2}$(red)(3) the couples have $E_{p,a} - E_{p,c}$ values in the range 140–90 mV, while for $E_{1/2}$(ox)(2) the values of $E_{p,a} - E_{p,c}$ are 170–200 mV. In all cases $i_{p,a} \approx i_{p,c}$. [c] $E_{1/2}$(red) values. [d] $E_{p,c}$ values.

Table V. Selected NMR Spectral Data for Dirhenium(III) Complexes of the Type $[Re_2(\mu\text{-}S)(\mu\text{-}X)X_2(CS)(\mu\text{-}LL)_2(NCR)]PF_6$ (X = Cl, Br; LL = dppm, dpam)[a]

complex	^1H NMR,[a] δ		$^{31}P\{^1H\}$ NMR,[d] δ
	RCN[b]	$-CH_2-$[c]	
$[Re_2(\mu\text{-}S)(\mu\text{-}Cl)Cl_2(CS)(dppm)_2(NCCH_3)]PF_6$	+2.98 s	+2.04 m, −0.08 m	−38.6, −75.2
$[Re_2(\mu\text{-}S)(\mu\text{-}Cl)Cl_2(CS)(dppm)_2(NCC_2H_5)]PF_6$	+3.42 q, +0.62 t	+1.84 m, −0.41 m	−44.0, −83.7
$[Re_2(\mu\text{-}S)(\mu\text{-}Cl)Cl_2(CS)(dppm)_2(NCC_6H_4\text{-}4\text{-}CH_3)]PF_6$	+2.70 s	+1.82 m, −0.38 m	−46.5, −86.1
$[Re_2(\mu\text{-}S)(\mu\text{-}Br)Br_2(CS)(dppm)_2(NCCH_3)]PF_6$	+2.85 s	+2.81 m, +0.36 m	−36.7, −69.6
$[Re_2(\mu\text{-}S)(\mu\text{-}Br)Br_2(CS)(dppm)_2(NCC_2H_5)]PF_6$	+3.43 q, +0.23 t	+2.42 m, +0.18 m	−41.3, −76.3
$[Re_2(\mu\text{-}S)(\mu\text{-}Br)Br_2(CS)(dppm)_2(NCC_6H_4\text{-}4\text{-}CH_3)]PF_6$	+2.70 s	+2.72 m, +0.14 m	−42.1, −77.3
$[Re_2(\mu\text{-}S)(\mu\text{-}Br)Br_2(CS)(dpam)_2(NCCH_3)]PF_6$	+3.05 s	+1.94 d, +0.24 d	
$[Re_2(\mu\text{-}S)(\mu\text{-}Br)Br_2(CS)(dpam)_2(NCC_2H_5)]PF_6$	+3.51 q, +0.57 q	+1.93 d, +0.23 d	

[a] Spectra recorded in CD_2Cl_2. [b] Resonances due to the aliphatic substituents on the nitrile ligand; s = singlet, t = triplet, q = quartet. [c] The $-CH_2-$ resonances of the dppm and dpam ligands. In the case of dppm these appear as an AB pattern with superimposed P–H coupling while for dpam they are doublets. [d] Spectra recorded in CH_2Cl_2 with aqueous H_3PO_4 as an external standard. The $^{31}P\{^1H\}$ NMR spectra have the appearance of AA′XX′ patterns; chemical shifts are those of the centers of the two multiplets.

ca. 20–30 cm^{-1} compared to their neutral precursors, in accord with an increase in the positive charge on the dimetal core and, consequently, a decrease in metal-to-CS(π^*) back-bonding. Also, the voltammetric half-wave potentials (Table IV) are shifted to more positive values to such an extent that the second oxidation $E_{1/2}$(ox)(2) is shifted beyond the potential limit of our measurements and a third reduction process ($E_{1/2}$(red)(3)) now becomes accessible.

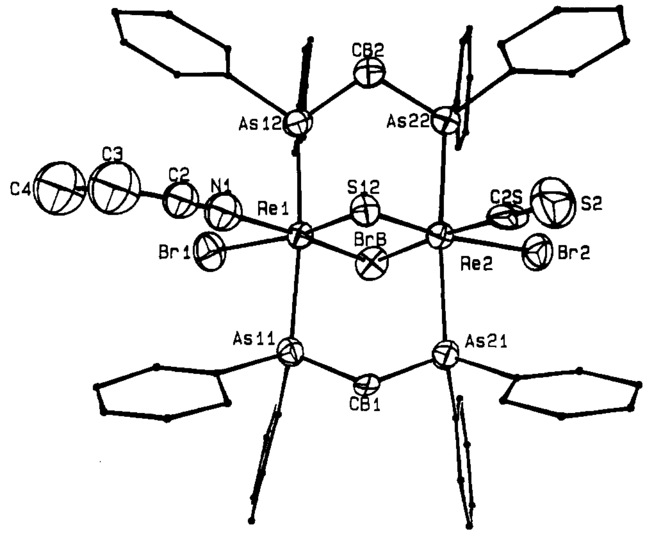

Figure 1. ORTEP representation of the structure of the $[Re_2(\mu\text{-}S)(\mu\text{-}Br)Br_2(CS)(\mu\text{-}dpam)_2(NCC_2H_5)]^+$ cation. The thermal ellipsoids are drawn at the 50% probability level except for the phenyl carbon atoms, which are drawn as circles of arbitrary radius.

The ^1H and $^{31}P\{^1H\}$ NMR spectral properties of the nitrile-containing derivatives of the type $[Re_2SX_3(CS)(LL)_2L']PF_6$ are presented in Table V. The appearance of the $^{31}P\{^1H\}$ NMR spectra as AA′XX′ patterns implies that these complexes, and their isocyanide analogues and neutral precursors, possess unsymmetric structures that are based upon edge-shared bioctahedra. This has been confirmed by X-ray crystallography. Although good quality single crystals of $Re_2SCl_4(CS)(dppm)_2$ were obtained from dichloromethane/hexane and a data set was collected at +20 °C, a complete and satisfactory refinement was thwarted by a disorder involving the chloride, sulfide, and CS ligands. However, a trans disposition of dppm ligands was shown to be present and the Re–Re distance found to be close to 2.9 Å. After several unsuccessful attempts, we eventually obtained a suitable crystal of one of the $[Re_2SX_3(CS)(LL)_2L']PF_6$ derivatives, specifically, the compound of composition $[Re_2SBr_3(CS)(dpam)_2(NCC_2H_5)]PF_6 \cdot CH_2Cl_2$. The pertinent crystallographic and structural data are presented in Tables I–III. The structure of the dirhenium cation, which contains the features identified in the preliminary structure determination of $Re_2SCl_4(dppm)_2$ (vide infra), is that of an edge-shared bioctahedron (Figure 1) with bridging bromide and sulfide ligands and a long Re–Re bond distance of 2.956 (2) Å. This distance is ca. 0.3 Å greater than those in authentic metal–metal-bonded dirhenium(III) complexes such as $Re_2(\mu\text{-}Cl)_2Cl_4(\mu\text{-}dppm)_2$[19] and in carbonyl-containing edge-shared bioctahedral species like $\mathrm{Re_2(\mu\text{-}Cl)(\mu\text{-}CO)Cl_3(\mu\text{-}dppm)_2(CO)}$,[20] both of which are prepared from $\mathrm{Re_2Cl_4(dppm)_2}$. The C–S distance of 1.40 (4) Å is within the range of 1.4–1.6 Å for terminally bound thiocarbonyl ligands,[1] and the Re–C–S unit is close to linear (174 (3)°).

Discussion

The formation of the complexes $\mathrm{Re_2(\mu\text{-}S)(\mu\text{-}X)X_3(CS)(\mu\text{-}LL)_2}$ (LL = dppm; dpam) and their closely related derivatives constitutes the first instances where a multiply bonded dimetal complex has brought about the 2-electron reduction of $\mathrm{CS_2}$ and where the CS and $\mathrm{S^{2-}}$ fragments have been incorporated into the resulting product in which the dimetal unit is preserved. Furthermore, this reactivity provides a convenient entry to the hitherto unknown sulfur-containing unit $\mathrm{[Re(\mu\text{-}S)(\mu\text{-}X)Re]^{n+}}$, where X is a halide ligand.

The most surprising result of the structure determination of $\mathrm{[Re_2(\mu\text{-}S)(\mu\text{-}Br)Br_2(CS)(\mu\text{-}dpam)_2(NCC_2H_5)]PF_6{\cdot}CH_2Cl_2}$ (**1**) was the unanticipated length of the Re–Re bond in an edge-shared bioctahedral dirhenium(III) complex of this type with two bridging dppm or dpam ligands.[15c,21] In compounds as disparate as the dirhenium(IV) complexes $\mathrm{(Ph_4P)_2[Re_2(\mu\text{-}S)_2(CN)_8]{\cdot}6H_2O}$[22] and $\mathrm{Re_2(\mu\text{-}S)_2[S_2CN(C_4H_9)_2]_4{\cdot}2THF}$[23] and the syn and anti forms of the dirhenium(VI) compound $\mathrm{Re_2(\mu\text{-}S)_2O_2(CH_2CMe_3)_4}$,[24] the Re–Re distances are 2.60 (no esd given), 2.546 (1), 2.759 (3), and 2.871 (2) Å, respectively, all of which are considerably shorter than that in **1**. This bond lengthening is also reflected in the rather large Re–S–Re angle of 82.1 (3)°; this compares with Re–S–Re angles of 68.1 (1)° in $\mathrm{Re_2(\mu\text{-}S)_2[S_2CN(C_4H_9)_2]_4{\cdot}2THF}$.[23] Note that the long Re–Re bond distance is not simply a consequence of the size of the bridging atoms (Br and S) since in the dirhenium(III) compounds $\mathrm{Re_2(\mu\text{-}SEt)_2Cl_4(dto)_2}$ (dto = 3,6-dithiaoctane)[25] and $\mathrm{Re_2(\mu\text{-}SePh)_2Cl_4(dppm)_2}$[26] the Re–Re bond distances are quite short (2.593 (1) and 2.656 (1) Å, respectively).

In spite of the relative structural complexity of the dirhenium cation in **1**, in particular the presence of two different anionic bridging ligands ($\mathrm{S^{2-}}$ and $\mathrm{Br^-}$), this compound fits between the extremes of the related edge-shared bioctahedral complexes $\mathrm{Re_2(\mu\text{-}Cl)_2Cl_4(dppe)_2}$ (dppe = $\mathrm{Ph_2PCH_2CH_2PPh_2}$), in which there is no metal–metal bond,[27] and the double bonded complex $\mathrm{Re_2(\mu\text{-}Cl)_2Cl_4(\mu\text{-}dppm)_2}$.[19,28] In the latter complex the ground-state configuration can be represented as $\sigma^2\pi^2\delta^{*2}\delta^2$ based upon an EHMO treatment,[28] which accords with the experimentally determined Re–Re bond distance of 2.616 (1) Å.[19] As the bridge angles begin to open up, as they do in the case of **1** where the Re–S–Re and Re–Br–Re angles are 82.1 (3)° and 70.57 (9)°, we can see from the Walsh diagram[28] for the model species $\mathrm{[Re_2(\mu\text{-}Cl)_2Cl_8]^q}$, where q represents the charge, that π^* can drop below δ. For a d^4–d^4 system such as **1**, the ground-state configuration could then become $\sigma^2\pi^2\delta^{*2}\pi^{*2}$ and give rise to a Re–Re bond order of <1. The destabilization of δ relative to π^* has its origin in the interaction of the former with the filled "nonbonding" orbitals on the bridging ligands. If this description of the electronic ground state for **1** is correct, then we would anticipate that upon oxidation to dirhenium(IV), as in the case of $\mathrm{[Re_2(\mu\text{-}S)_2]^{4+}}$ complexes,[22,23] the Re–Re bond order would increase to approximate a Re=Re bond; this accords with the measured Re–Re bond distances of ca. 2.6 Å.[22,23]

Acknowledgments. Support from the National Science Foundation, through Grant No. CHE88-07444 to R.A.W., is gratefully acknowledged. We also thank the National Science Foundation (Grant No. CHE86-15556) for funds for the purchase of the MicroVAX II computer and diffractometer and the National Institutes of Health (Grant No. RR-01077) and the National Science Foundation (Grant No. 8714258) for funds for purchase of the NMR spectrometers.

Supplementary Material Available: Tables giving full details of the crystal data and data collection parameters (Table S1), the positional parameters for all atoms (Table S2), the thermal parameters (Table S3), and complete bond distances and bond angles (Tables S4 and S5) for $\mathrm{[Re_2(\mu\text{-}S)(\mu\text{-}Br)Br_2(CS)(\mu\text{-}dpam)_2(NCC_2H_5)]PF_6{\cdot}CH_2Cl_2}$ (15 pages); a table of observed and calculated structure factors (17 pages). Ordering information is given on any current masthead page.

---

(19) Barder, T. J.; Cotton, F. A.; Lewis, D.; Schwotzer, W.; Tetrick, S. M.; Walton, R. A. *J. Am. Chem. Soc.* **1984**, *106*, 2882.

(20) Cotton, F. A.; Daniels, L. M.; Dunbar, K. R.; Falvello, L. R.; Tetrick, S. M.; Walton, R. A. *J. Am. Chem. Soc.* **1985**, *107*, 3524.

(21) Price, A. C.; Walton, R. A. *Polyhedron* **1987**, *6*, 729.

(22) Laing, M.; Bregeault, J.-M.; Griffith, W. P. *Inorg. Chim. Acta* **1978**, *26*, L27.

(23) Wei, L.; Halbert, T. R.; Murray, H. H., III; Stiefel, E. I. *J. Am. Chem. Soc.* **1990**, *112*, 6431.

(24) Cai, S.; Hoffman, D. M.; Wierda, D. A. *Inorg. Chem.* **1991**, *30*, 827.

(25) Heyen, B. J.; Powell, G. L. *Inorg. Chem.* **1990**, *29*, 4574.

(26) Cotton, F. A.; Dunbar, K. R. *Inorg. Chem.* **1987**, *26*, 1305.

(27) Jaecker, J. A.; Robinson, W. R.; Walton, R. A. *J. Chem. Soc., Dalton Trans.* **1975**, 698.

(28) (a) Shaik, S.; Hoffman, R. *J. Am. Chem. Soc.* **1980**, *102*, 1194. (b) Shaik, S.; Hoffmann, R.; Fisel, C. R.; Summerville, R. H. *J. Am. Chem. Soc.* **1980**, *102*, 4555.